Letter

Lorentz-invariant topological structures of the electromagnetic field in a Fabry-Perot resonant slit grating

Marina Yakovleva [*], Jean-Luc Pelouard, and Fabrice Pardo [†]
Université Paris-Saclay, CNRS, Centre de Nanosciences et de Nanotechnologies, 91120, Palaiseau, France

(Received 25 August 2022; accepted 15 November 2022; published 7 December 2022)

It is commonly assumed that the most correct description of the electromagnetic world is the abstract one, and that topological constructs, such as lines of force are not covariant. In this Letter, we show that for a y-invariant system with a p-polarized electromagnetic field, it is possible to construct absolute (i.e., Lorentz invariant) lines in (t, x, z) space-time, which we call *electric spaghettis* (ESs). The electromagnetic field is fully described by the ES topology that transcends the limit between space and time, plus a new invariant, the characteristic parameter η. In a Fabry-Perot resonant slit grating, three ES patterns can be distinguished, corresponding to three regions: null straight lines in plane-wave regions, rounded rhombi in the interference region inside the grating, and Bernoulli's logarithmic spiral patterns—the first ever described fractals—in the funneling region.

DOI: 10.1103/PhysRevA.106.L060201

Faraday's concept of lines of force [1,2] was the first topology describing the electromagnetic field. However, with our modern point of view, this topological construct is not Lorentz invariant, and it is commonly assumed that *the most correct description of the electromagnetic field is the abstract one* [3,4]. Nevertheless, few attempts to define a space-time topology of the electromagnetic field have been performed. The idea of tubes of flux, a space-time generalization of Maxwell's concept [2], was described, for example, by Misner *et al.* in their book *Gravitation* [5]. Unfortunately, it only leads to a schematic and does not construct well-defined space-time topological structures. A frequent approach of field two-forms is to separate space and time [6,7], losing the Lorentz invariance. Absolute representations of two-forms were given only for simple cases, by Jancewicz for an electric charge [8] and by Warnick and Russer for the case of a propagating plane wave [9].

In an attempt to construct a Lorentz-invariant topology of the electromagnetic field, Gratus [10] has suggested to consider fixed-coordinate space slices of the four-dimensional (4D) space-time. A space slice, being arbitrary in the general case, is canonical for a y-invariant p-polarized electromagnetic field. In this case, the Maxwell's two-form becomes a simple two-form, and its pullback onto any arbitrary $y =$ Const plane defines lines in the two- plus one-dimensional (2+1D) space-time. There is similarity between these lines and Faraday's lines of force for a static field in three-dimensional (3D) space. The topology by itself defines at any point (or event) two directional parameters, and a third parameter is necessary to completely describe the field, either the value of the electrostatic potential or the field amplitude (that can be illustrated by the density of lines). However, this field description by a topology plus a parameter cannot be straightforwardly generalized from 3D space to $2 + 1$D space-time, mainly because of the peculiarity of null-like directions in the latter. In the absence of charge, it is evident that field lines never end in 3D space, but this is not an established fact in $2 + 1$D space-time.

In this Letter, we show that a y-invariant p-polarized electromagnetic field (i.e., satisfying the Maxwell's and constitutive equations) can be fully described by an absolute topology of lines in (t, x, z) space-time [named here the *electric spaghettis* (ESs)] with a new Lorentz-invariant scalar measure on them, the η parameter. This topology is studied in detail for an infinite line of charge and for a Fabry-Perot resonant slit grating. The latter exhibits three specific topological ES structures: the single plane-wave region high above the grating, the two interfering plane-wave regions inside the grating, and the funnel region in the near field of the grating. In the funneling region a fractal topological structure around null field events is observed. These endless ES whirls, which seem to contradict the absence of magnetic charge [10], are justified here by a careful analysis.

For a y-invariant p-polarized field, the six components of Faraday's $F = (\boldsymbol{-E}, \boldsymbol{B})$ or Maxwell's $\mathcal{G} = (\boldsymbol{H}, \boldsymbol{D})$ 2-forms [5,11] reduce to three components with

$$\mathcal{G} = H_y dt \wedge dy + D_x dy \wedge dz + D_z dx \wedge dy, \tag{1}$$

in natural units ($c = 1$). Factoring out dy, this 2-form can be written as $\mathcal{G} = \phi_e \wedge dy$ with ϕ_e the 1-form

$$\boldsymbol{\phi}_e = H_y dt + D_z dx - D_x dz. \tag{2}$$

The dual of this 1-form is the vector,

$$\boldsymbol{\tau}_S = H_y \partial_t - D_z \partial_x + D_x \partial_z. \tag{3}$$

This vector defines integral curves, the ESs, that are absolute topological structures in $2 + 1$D space-time: a given line connects the same set of events, independently of any frame of reference. A tensorial approach and the explicit Lorentz transform calculation is given in the Supplemental Material

[*]marina.yakovleva@c2n.upsaclay.fr
[†]fabrice.pardo@c2n.upsaclay.fr

[12]. Starting from from any event $\boldsymbol{s}_0$, the line $\mathrm{ES}(\boldsymbol{s}_0)$ can be built using the parametric equation,

$$\boldsymbol{s}(\eta) = \boldsymbol{s}_0 + \int_0^{\eta} \boldsymbol{\tau}_S d\eta. \tag{4}$$

The 2-form Eq. (1) that allows to compute the electric flux $\mathcal{G}(\sigma)$ on any oriented surface element σ in 3 + 1D space-time (with a density D_x on $\partial_y \wedge \partial_z$ surface, D_z on $\partial_x \wedge \partial_y$ surface, and H_y on $\partial_t \wedge \partial_y$ surface), reduces to the 1-form $\boldsymbol{\phi}_e$, which, being applied to any vector $\boldsymbol{a}$ in 2 + 1D space-time, gives the electric flux value $\varphi_e(\boldsymbol{a}) = \mathcal{G}(\boldsymbol{a} \wedge \partial_y)$ on this vector. The electric flux on a spaghetti segment $\mathrm{ES}_{e_1e_2}$ from the event $\mathrm{e}_1 = \boldsymbol{s}(\eta_1)$ to the event $\mathrm{e}_2 = \boldsymbol{s}(\eta_2)$ has then the value,

$$\varphi_e(\mathrm{ES}_{e_1e_2}) = \int_{\eta_1}^{\eta_2} (H^2 - D^2) d\eta. \tag{5}$$

In this equation, the electric flux value φ_e and the $H^2 - D^2$ factor are both Lorentz invariant. Hence, $\eta(\mathrm{ES}_{e_1e_2}) = \eta_2 - \eta_1$ is actually a new Lorentz invariant.

From a topological point of view, a set of ESs can be constructed to cover any region of the 2 + 1D space-time with a nonzero electromagnetic field. Furthermore, an oriented segment of ES can be labeled with three quantities: (1) its interval length (but only if the segment is purely timelike or spacelike), (2) its electric flux φ_e, and (3) its characteristic parameter η.

Unlike world lines of physical objects, which are always timelike, ESs transcend the boundary between time and space directions. Some parts of the same ES can be timelike, spacelike, and even lightlike. The particular case where ESs are contained in a light cone requires some attention as $H^2 - D^2$, the interval and the electric flux are all equal to zero. In contrast, the η value of a nondegenerate (i.e., not reduced to a point) ES segment is never zero, and has a sign fixed by the orientation of ES. If an arbitrary inertial frame of reference is chosen, the components of the electromagnetic field can be obtained from the ES topology and the η value using Eq. (4),

$$H_y = \frac{ds_t}{d\eta}, \quad D_z = -\frac{ds_x}{d\eta}, \quad D_x = \frac{ds_z}{d\eta}, \tag{6}$$

where s_t, s_x, s_z are the ES coordinates. The smaller the field, the larger the η value. It may seem rather counterintuitive, but the ES characteristic parameter η is an absolute extensive physical property of ESs.

Figure 1(a) shows the case of a linear constant density of charge λ along the y direction. The world line of each charge is a straight line along the Ot axis, and this axis represents all charges in 2 + 1D space-time (t, x, z). ESs appear as concentric green circles centered around the Ot line. Every ES circle contains the same electric flux value $\varphi_e = \lambda$. The pink radial surfaces are zero-electric flux surfaces (ZEFSs). They are perpendicular to the ESs and start on the Ot charge world line. The electric flux on them is zero.

At first glance, Fig. 1(a) is a picture of equipotential lines (green circles, which are indeed cylinders along the y axis in 4D space-time) and electric-field strength lines, extended in the time direction (pink surfaces). However, the concept of equipotential lines is frame dependent: in a different frame of reference, a magnetic field would appear, and both the electric field and the equipotential lines would change. In contrast, ESs and ZEFSs are absolute, connecting the same

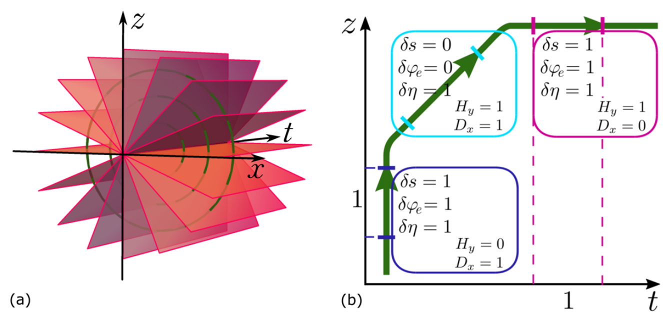

FIG. 1. (a) A t-invariant (electrostatic) case: an Oy charged line with the Ot world line. Green circles: ESs and pink surfaces: ZEFSs. (b) A non-t-invariant case: ES (green line) with purely an electric-field part (z direction, dark-blue frame), plane-wave part (null-like direction, light-blue frame), and purely magnetic field (t direction, purple frame). The ES topology is absolute, the interval values δs, the flux values $\delta\varphi_e$, and the characteristic parameter values $\delta\eta$ are all absolute, independent of the reference frame. In contrast, H_y and D_x depend on the axis choice (t, z) with Eqs. (3) and (6). When ES is null-like, only the parameter η has a nonzero value, able to describe the electromagnetic field in this region.

set of events, independently of any frame of reference. The η value calculated between two events of a given ES is absolute, independent of the choice of a reference frame. The field components, which are relative, can be simply derived from the ES topology and the parameter η, using Eq. (6). In this electrostatic example, φ_e has the same value λ on all circles. By contrast, $\eta = 4\pi^2 R^2/\lambda$ is proportional to the square of the radius R. The usefulness of the parameter η, not obvious in this example, is crucial when the ES part belongs to a light cone as shown in Fig. 1(b) where an ES is successively spacelike, null-like, and timelike, transcending the distinction between space and time.

The Fabry-Perot resonant slit grating system studied in this Letter consists of a perfectly conducting metal with slits parallel to the y direction [Fig. 2(a)], excited at normal incidence by a p-polarized plane wave (i.e., with the magnetic field oriented along the y direction). The grating period is $L = \pi$, that is, half the wavelength $\Lambda = 2\pi$ $(c = 1)$, so all the diffracted waves are evanescent. The slit width is arbitrarily chosen as $w = L/6$. This system is known for perfect transmission of incident radiation [13] with a funneling mechanism [Fig. 2(b)] that can be understood by the magnetoelectric interference between the incident and the evanescent fields [14]. The Fabry-Perot resonance condition corresponding to total transmission and no reflection is obtained for a slit height h equal to $h = h_0 + n\,\Lambda/2$ with $h_0 \approx 0.417\Lambda$, and n is an arbitrary integer. The value of h_0 is slightly smaller than $\Lambda/2$ as the phase of the internal reflection is not exactly π. The value of $h = 0.917\Lambda$ was chosen for a clear view of the interference pattern inside the slits.

Several numerical techniques based on Eqs. (4) and (5) were used to compute ESs and ZEFSs. Full descriptions of these and code books are presented in the Supplemental Material [12]. Figure 2(d) shows ESs crossing the line $z = -h/2, x = -2w/5$. The median plane of a slit is a special place because the D_z component is here equal to zero, and the ESs remain localized on this plane [see Eq. (3) and Fig. 2(c)].

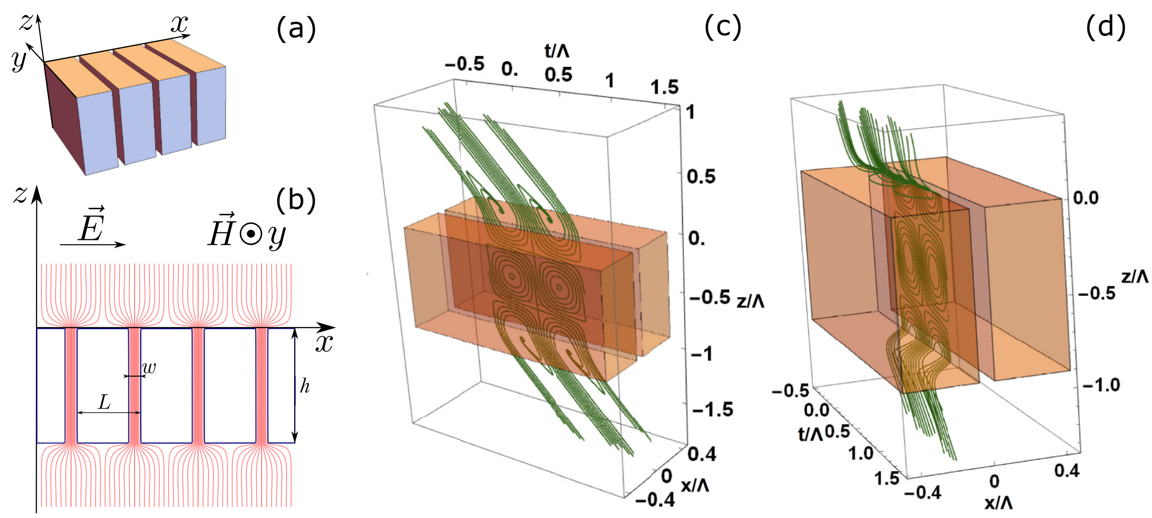

FIG. 2. (a) Slit grating, invariable in the y direction, made in a perfect conductor. (b) Time-averaged Poynting vector lines in the resonant case, p-polarized normally incident monochromatic wave. (c) ESs in the central plane of a slit. (d) ESs crossing the line $z = -h/2$, $x = -2w/5$.

These ESs are also plotted in Fig. 3 along with ZEFS lines. As there are no electric charges in the considered region, the electric flux is constant between two neighboring bold ZEFS lines, and the density of these lines in the t direction corresponds to the value of the field component H_y, and the density in the z direction corresponds to the value of the field component D_x.

Far from the slits where a single plane wave propagates $D_x = H_y$, the ESs are straight null-like lines according to Eq. (3). Inside a slit where two plane waves interfere, concentric patterns of rounded rhombi are observed. The field is purely electric when the ESs (green lines) are parallel to the z direction and purely magnetic when they are parallel to the t direction. Owing to the resonance inside the slit, the electric flux density in this region is six times higher than on the plane-wave region. This is clearly depicted in Fig. 3: in the slit region, there are six ZEFS lines over a half-period in time, whereas in the upper part of the figure (plane-wave region), there is only one bold ZEFS line. Compared with the interference of two identical plane waves [15], the rounded squares are slightly distorted. This is because the amplitude of the wave from bottom to top is smaller than that from top to bottom.

In the funneling region, ESs form whirls that are centered on zero field events. They seem to contradict the principle that tubes of flux with no charge never end [5], so they require detailed analysis. The field in the funneling region is the superposition of the incoming plane wave and of a series of diffracted evanescent waves. For simplicity, let us restrict the continuation of the study to only the first diffracted wave. In this model, the incident plane wave has amplitude $\cos(z+t)$, and the evanescent wave has amplitude $a\exp(-\sqrt{3}z)\sin(t)\cos(2x)$ where the amplitude $a = 1.091$ and the phase $\pi/2$ are obtained numerically (see the Supplemental Material [12]). The ES-ZEFS pattern of this interference is plotted as, respectively, green and red lines in Fig. 4(a). The pattern of this simplified model is similar to the

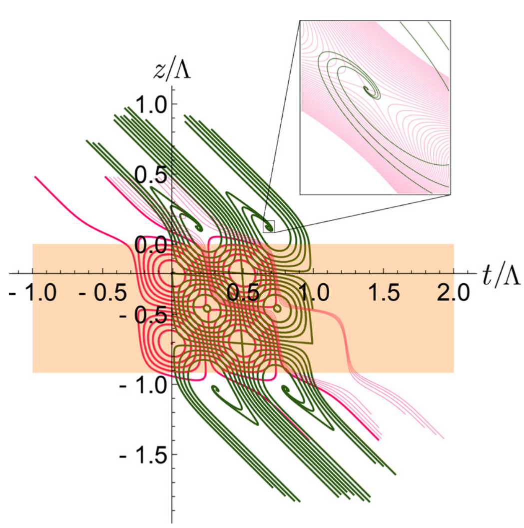

FIG. 3. Plot of the ES (green) and ZEFS (red) lines on the median plane for one time period. The orange zone corresponds to the slit area. The electric flux is constant between two thick red ZEFS lines and between two thin red lines with a factor of 1/6. The inset: zoom of the whirl zone with very small flux steps between ZEFS lines.

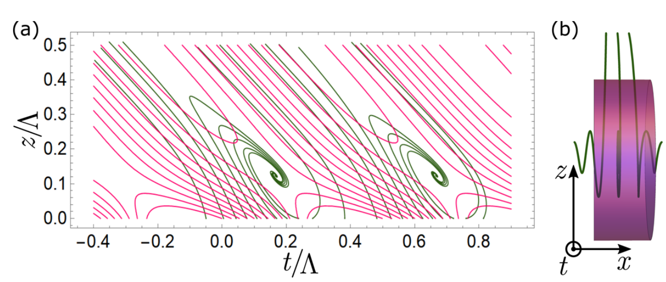

FIG. 4. (a) ESs (green) and ZEFS lines (red) in the case of interference of the plane wave and two evanescent ones (with equal amplitudes and opposite propagation directions along the x axis). (b) Space-time camembert box (also known as a pill box) with incoming, never outgoing ESs at $x = 0$. Other ESs are outgoing through one of the sides.

one observed in Fig. 3. The whirls are centered on zero-field points $H_y = D_x = 0$.

Using a linear approximation of the field components around the zero-field points ($t_0 = \pi/3 + p/2,\ z_0 = 0.7736$), the parametric equation of an ES is (see the Supplemental Material [12]),

$$\begin{pmatrix} t(\eta) - t_0 \\ z(\eta) - z_0 \end{pmatrix} = z_0 \begin{pmatrix} 0 & \beta \\ 1 & -\alpha \end{pmatrix} \begin{pmatrix} \cos \lambda_i \eta \\ \sin \lambda_i \eta \end{pmatrix} e^{-\lambda_r \eta}, \tag{7}$$

$$x(\eta) = x_0 e^{2\lambda_r \eta}, \tag{8}$$

where $\lambda_i = \sqrt{(3 \sin z_0 + \frac{\cos z_0}{\sqrt{3}})(\sin z_0 - \frac{\cos z_0}{\sqrt{3}})}$, and $\lambda_r = \sin z_0 - \frac{\cos z_0}{\sqrt{3}}$. For $x_0 = 0$ this is an affine transformation of a curve, named *spira mirabilis* by Bernoulli three centuries ago [16]. It is an endless spiral, the first fractal curve ever studied. And this is the key of the paradox that ESs should never end. They never end indeed. Each loop of the ES toward the center corresponds to $2\pi/\lambda_i$ change in the parameter η whereas the radius decreases by a factor of $\exp(-2\pi\lambda_r/\lambda_i) = 0.12$.

The ES bundles in a vacuum makes tubes of magnetic flux, corresponding to the Faraday 2-form $E_x dx \wedge dt + E_z dz \wedge dt + B_y dz \wedge dx$ (see the Supplemental Material [12]). As there are no magnetic charges, any tube entering on a given closed surface Σ of space-time (t, x, z) must exit somewhere on the same surface. The observed endless ESs do not contradict this law because they are restricted to $x = 0$ plane, having zero measure on the surface Σ. Considering the camembert box (also known as the pill box) in Fig. 4(b), the incoming ESs at the periphery exit through the sides of the disk, thus, defining tubes of constant magnetic flux.

To conclude, we demonstrated that a y-invariant p-polarized electromagnetic field, which is usually represented by three field components (as H_y, D_z, D_x, relative to a frame of reference), can be represented in an absolute way. In a flat space-time, the qualifier *absolute* is synonymous with the *Lorentz invariant*. It should be noted that the content of this Letter can be extended to a curved space-time, provided that there is translation symmetry along the y direction. The electromagnetic field can be represented by unique and absolute structures, the Ss, measured by the absolute parameter η. The surfaces perpendicular to ESs (the ZEFSs) are also absolute space-time structures. Contrary to the world lines of physical objects, which are always timelike, ESs and ZEFSs transcend the limit between space and time. Any segment of ES is characterized by two absolute electromagnetic quantities: its electric flux φ_e, and its characteristic parameter η. Despite its counterintuitive nature (the larger it is, the smaller the field is), η is a parameter that makes sense because it can describe the electromagnetic field everywhere. In contrast, the flux and interval values, which are zero on null-like segments of ESs, cannot describe the electromagnetic field everywhere. ESs with η milestones written on them form a complete representation of the electromagnetic world in the 2 + 1D y-invariant space-time, giving in any inertial frame of reference (t, x, z), the field components H_y, D_z, D_x.

We explored the ES topology of a Fabry-Perot resonant slit grating. In the plane-wave region ESs are straight light lines with an electric field equal to the magnetic field. Inside the slits, the ESs are mainly rounded rhombi, corresponding to the interference of two plane waves with purely H_y zones and purely D_x zones. The funneling region is of particular interest with ESs having the fractal behavior of logarithmic spirals. They correspond to the interference of the incident wave with the evanescent waves diffracted by the slit grating.

ESs illustrate the profound unity of electric and magnetic fields and give them a topological structure that can be studied for itself, opening a new field of research. Also, instead of considering field components, which are related to an arbitrary frame of reference, the description of the field as an absolute topology in space-time with absolute measure η is a radical change in the conceptual approach to the electromagnetic world. This not only has philosophical and educational consequences, but also suggests new computational approaches.

[1] M. Faraday, London, Edinburgh, and Dublin Philos. Mag. J. Sci. **3**, 401 (1852).

[2] J. C. Maxwell, London, Edinburgh, and Dublin Philos. Mag. J. Sci. **21**, 161 (1861).

[3] R. P. Feynman, R. B. Leighton, and M. Sands, *The Feynman Lectures on Physics: Mainly Electromagnetism and Matter* (Addison-Wesley, Reading. reprinted, 1977), Vol. 2.

[4] F. Dyson, in *The Second European Conference on Antennas and Propagation, EuCAP 2007* (EICC, Edinburgh, UK, 2007), pp. 1–6, doi: 10.1049/ic.2007.1146.

[5] C. W. Misner, K. S. Thorne, and J. A. Wheeler, *Gravitation* (W. H. Freeman, Princeton University Press, 1973).

[6] G. A. Deschamps, Proc. IEEE **69**, 676 (1981).

[7] K. F. Warnick and P. H. Russer, Prog. In Electromag. Res. **148**, 83 (2014).

[8] B. Jancewicz, *Multivectors and Clifford Algebra in Eectrodynamics* (World Scientific, Singapore, 1989).

[9] K. F. Warnick and P. Russer, Turkish J. Electrical Eng. Comput. Sci. **14**, 153 (2006).

[10] J. Gratus, arXiv:1709.08492.

[11] A. Stern, Y. Tong, M. Desbrun, and J. E. Marsden, Geometric computational electrodynamics with variational integrators and discrete differential forms, in *Geometry, Mechanics, and Dynamics*, Fields Institute Communications, Vol. 73, edited by D. Chang, D. Holm, G. Patrick, and T. Ratiu (Springer, New York, NY, 2015), pp. 437–475, doi:10.1007/978-1-4939-2441-7_19.

[12] See Supplemental Material at http://link.aps.org/supplemental/10.1103/PhysRevA.106.L060201 for detailed calculations and proofs.

[13] P. N. Stavrinou and L. Solymár, Opt. Commun. **206**, 217 (2002).

[14] F. Pardo, P. Bouchon, R. Haïdar, and J.-L. Pelouard, Phys. Rev. Lett. **107**, 093902 (2011).

[15] F. Pardo, in *Séminaire Général du Département de Physique* (École Polytechnique, Palaiseau, France, 2016), https://youtu.be/PAne0N6PtI8.

[16] Ø. Hammer, *The Perfect Shape* (Springer, Berlin, 2016), pp. 33–38.